ELSEVIER

Polymer 42 (2001) 6019–6030

polymer

www.elsevier.nl/locate/polymer

Synthesis and characterization of novel polyimides containing fluorine and phosphine oxide moieties

K.U. Jeong, J.-J. Kim, T.-H. Yoon*

Department of Materials Science and Engineering, Kwangju Institute of Science and Technology, 1 Oryong-dong, Buk-gu, Kwangju, 500-712, South Korea

Received 18 July 2000; received in revised form 18 October 2000; accepted 27 November 2000

Abstract

A novel diamine monomer, containing fluorine and phosphine oxide, bis(3-aminophenyl)-3,5-bis(trifluoromethyl)phenyl phosphine oxide (mDA6FPPO), was prepared via Grignard reaction from diphenylphosphonic chloride and 3,5-bis(trifluoromethyl)bromobenzene. First, 3,5-bis(trifluoromethyl)phenyl diphenyl phosphine oxide (6FPPO) was prepared and subjected to nitration and reduction to obtain mDA6FPPO. The monomers were characterized by FT-IR, ^{1}H-NMR, ^{31}P-NMR, ^{19}F-NMR, titrator and elemental analyzer (EA). The monomer was then utilized to prepare polyimides with dianhydrides such as 6FDA, BTDA, ODPA or PMDA by the conventional two-step method; preparation of poly(amic acid), followed by solution imidization. The polyimides were characterized by FT-IR, NMR, DSC and DMA, with intrinsic viscosity, refractive index and adhesive properties also being evaluated. A phosphine oxide containing monomer, bis(3-aminophenyl) phenyl phosphine oxide (mDAPPO) and a commercial 3,3′-diaminodiphenylsulfone (mDDS) were also used for comparison. The polyimides with mDA6FPPO exhibited high T_g (228–281°C), good thermal stability, very low birefringence (0.001) and good adhesive properties. © 2001 Elsevier Science Ltd. All rights reserved.

Keywords: Polyimide; Phosphine oxide; Birefringence

1. Introduction

Aromatic polyimides have been utilized in electronic packaging applications for the past decade due to their excellent dielectric, thermal, adhesive and mechanical properties, chemical resistance, and dimensional stability [1–4]. Among these, the low dielectric constant is one of the decisive factors in minimizing electrical power loss and delay of signal transmission in thin film insulators [5,6], thus allowing smaller and lighter electronic devices. Such stringent requirements have led to extensive investigation of fluorination [7–17] and nanofoam technology [18–21] and more recently, the utilization of organic–inorganic hybrid nanocomposites and poly(silsesquioxane) have been introduced [22,23].

The unique characteristics of fluorine, such as high electronegativity, low polarity, and low cohesive and surface free energy led Critchley to attempt the fluorination of polyimide in 1972 [24]. Since then, fluorine-containing diamines and dianhydrides have been introduced to prepare fluorinated polyimdes with properties of low water up-take, low reflective index and low dielectric constant [7–17]. Fluorination is also known to enhance the solubility of polyimides even in chloroform, toluene or tetrachloroethane (TCE), even with full imidization [7,25]. However, fluorinated polyimides also have drawbacks such as poor adhesion, low mechanical strength and high coefficient of thermal expansion (CTE) [7]. This has led to the introduction of polyimide nanofoam. The polyimide nanofoam was prepared by generating nano-size air pockets in the polyimide film by degrading the labile blocks such as polypropylene oxide [18–21]. Since the dielectric constant of air is approximately one, the polyimide nanofoam could provide much lower dielectric constant than that of polyimide. Unfortunately, a major disadvantage of the nanofoam is the high processing temperature in air needed to pyrolyze the labile blocks, which oxidizes the Cu circuit.

Although polyimides have good adhesive properties, much effort has been directed towards further improvement of adhesion in order to enhance the reliability of electronic devices, especially for fluorinated polyimides [7,26]. Adhesion promoters such as silane-coupling agents were widely utilized to improve adhesion, but these also have adverse effect on the performance of devices. Moreover extra processing steps can increase the processing cost [27,28]. On the other hand, phosphine oxide containing polyimides and polysulfones are also known to have excellent adhesive

---

* Corresponding author. Tel.: +82-62-970-2307; fax: +82-62-970-2304.
E-mail address: thyoon@kjist.ac.kr (T.-H. Yoon).

0032-3861/01/$ - see front matter © 2001 Elsevier Science Ltd. All rights reserved.
PII: S0032-3861(01)00012-X

properties [29–31] with the added benefits of excellent thermal stability [31] and miscibility owing to strong hydrogen bonding [32]. It was also reported that triphenyl phosphine oxide moieties in the polyimide have non-coplanar structure [29] possibly providing low birefringence.

Therefore, in this study, a novel diamine monomer containing phosphine oxide and fluorine, bis(3-aminophenyl)-3,5-bis(trifluoromethyl)phenyl phosphine oxide (mDA6FPPO), was prepared via the Grignard reaction and utilized to synthesize polyimides with low dielectric constant, good thermal and adhesive properties, and solubility. Polyimides were synthesized by the conventional two-step method; preparation of poly(amic acid) followed by solution imidization, with the molecular weight controlled to 20,000 g/mol by off setting the stoichiometry and adding phthalic anhydride. The polymers were subjected to thermal, optical and adhesive property measurements, and compared to polyimides prepared from phosphine oxide containing diamine monomer, bis(3-aminophenyl)-phenyl phosphine oxide (mDAPPO), and a commercial monomer, 3,3′-diaminodiphenyl sulfone (mDDS).

2. Experimental

2.1. Materials

Diphenylphosphinic chloride (98%), 3,5-bis(trifluoromethyl)bromobenzene (99%), triphenylphosphine oxide (98%), Mg turnings, sulfuric acid and nitric acid were obtained from Aldrich and used as-received. Phthalic anhydride (99%), also purchased from Aldrich was vacuum sublimed twice prior to use. *N*-methylpyrrolidinone (NMP) and 1,2-dichlorobenzene (*o*-DCB) obtained from Fisher, were stirred over P_2O_5 (phosphorus pentoxide) overnight, and then vacuum distilled. *N*,*N*-dimethylacetaimide (DMAc), toluene, absolute ethyl alcohol and chloroform from Fisher, as well as tetrachloroethane (TCE) from Yakuri, Japan were used as received. Tetrahydrofuran (THF, Aldrich) was purified by distillation after stirring over calcium hydride.

Bis(3-aminophenyl)-3,5-bis(trifluoromethyl)phenyl phosphine oxide (mDA6FPPO), containing fluorine and phosphine oxide moiety was synthesiszed in our laboratory and used to prepare polyimides. A monomer containing only phosphine oxide, bis(3-aminophenyl)phenyl phosphine oxide (mDAPPO) as reported in the literature [33] and 3-aminophenyl sulfone (mDDS) from Aldrich were utilized for comparison. All anhydrides such as pyromellitic dianhydride (PMDA), 3,3′,4,4′-benzophenone tetracarboxylic dianhydride (BTDA), 5,5′-[2,2,2-trifluoro-1-(trifluoromethyl)-ethyliden]-bis-1,3-isobenzofuranedione (6FDA), and 4,4′-oxydiphthalic dianhydride (ODPA) were obtained from Chriskev and used as received. Cu foils (0.035 mm in thickness, bare and Cr/silane coated) were provided by Iljin, Korea.

2.2. Synthesis of 3,5-bis(trifluoromethyl)phenyl diphenyl phosphine oxide

3,5-Bis(trifluoromethyl)phenyl diphenyl phosphine oxide (6FPPO) was synthesized via the Grignard reaction (Scheme 1 (synthesis of bis(3-aminophenyl)-3,5-bis(trifluoromethyl)phenyl phosphine oxide (mDA6FPPO))). Thus, 4.23 g (0.1746 mol) of Mg turnings (99%) and 120 ml of purified THF were charged into a flame-dried

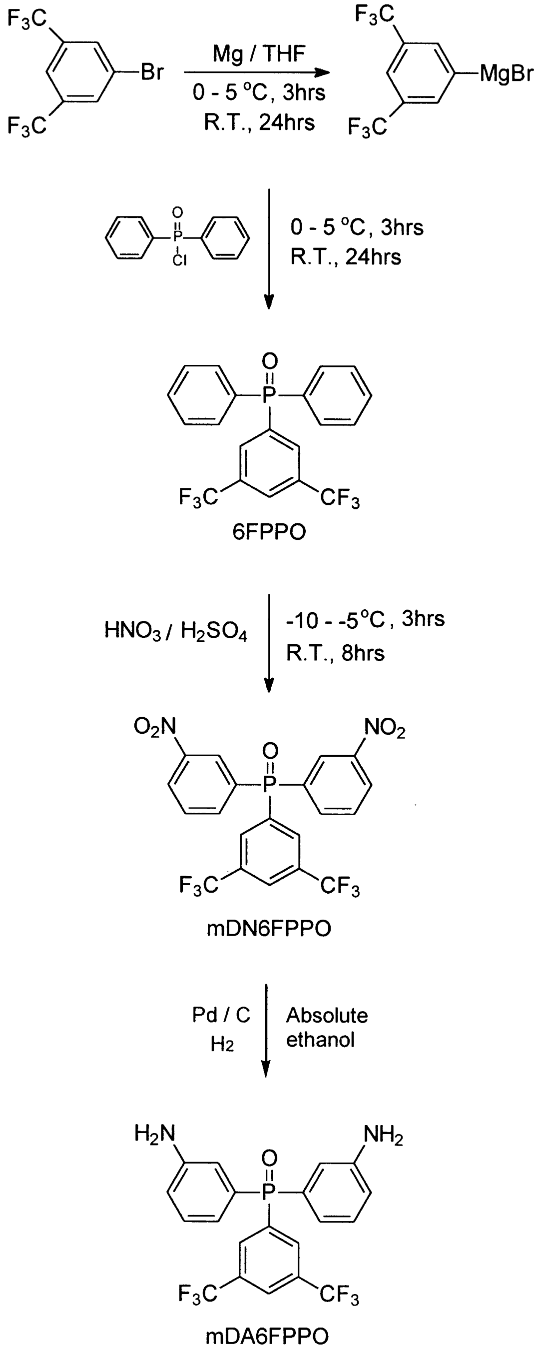

Scheme 1.

500 ml three-neck round bottom flask, equipped with magnetic stirrer, addition funnel, condenser, drying tube, thermometer and nitrogen inlet. The solution was first cooled to below 5°C in an ice bath, then 23.5 ml (0.1346 mol) of 3,5-bis(trifluoromethyl)bromobenzene (99%) was added dropwise over a period of 3–4 h, while stirring vigorously. The mixture was allowed to react overnight, while the temperature of the reaction mixture reached r.t. as the ice in the bath slowly melted. The ice was again added to the bath to afford 5°C or lower and 23.5 ml (0.1207 mol) diphenylphosphinic chloride (98%) was added dropwise over 3–4 h. After reacting for another 24 h, a brown solution was obtained.

Next, 10% aqueous sulfuric acid was added to the solution to obtain a pH of 1, followed by the addition of 1 l of water and diethyl ether to form an aqueous layer and an organic layer. After decanting the organic layer, the aqueous layer was washed twice with diethyl ether and all organic parts were collected and dried by evaporation, resulting in 6FPPO, a light brown solid. This was dissolved in chloroform and washed several times with 10% sodium bicarbonate and three times with water. The organic part was condensed by a rotary evaporator, followed by precipitation into 2 l of boiling hexane. After hot filtration, the solution was condensed by rotary evaporator and stored at room temperature for 12 h and another 12 h in a freezer. The fibrous off-white crystals were collected by vacuum filtration and further purified by recrystallization in hexane (yield: 85%).

2.3. Preparation of bis(3-nitrophenyl)-3,5-bis(trifluoromethyl)phenyl phosphine oxide

Bis(3-nitrophenyl)-3,5-bis(trifluoromethyl)phenyl phosphine oxide (mDN6FPPO) was prepared by the nitration of 3,5-bis(trifluoromethyl)phenyl diphenyl phosphine oxide (6FPPO) using sulfuric acid and nitric acid (Scheme 1). Purified 6FPPO (30 g, 0.0724 mol) was added into 1 liter three-neck flask equipped with an addition funnel, nitrogen inlet, thermometer, drying tube and mechanical stirrer. Concentrated sulfuric acid (300 ml) were charged to produce an approximately 10 wt.% solids concentration. After completely dissolving 6FPPO at room temperature, the solution was cooled to −5°C with an ice–salt-water bath. Fuming nitric acid (14 ml) in 43 ml of sulfuric acid was added dropwise to the solution over a period of 3 h, while stirring vigorously and maintaining −5°C. The mixture was allowed to react for 8 h without adding more ice, then poured into 2 kg of finely divided ice. The resulting yellowish oil was extracted with chloroform, followed by washing with sodium bicarbonate aqueous solution until pH reached 7. The solvent was removed with a rotary evaporator and the remaining solid was crystallized twice from absolute ethanol, which afforded 34.5 g of pale yellow crystals, mDN6FPPO (yield:95%).

2.4. Preparation of bis(3-aminophenyl)-3,5-bis(trifluoromethyl)phenyl phosphine oxide

Bis(3-aminophenyl)-3,5-bis(trifluoromethyl)phenyl phosphine oxide (mDA6FPPO) was obtained by hydrogenation of bis(3-nitrophenyl)-3,5-bis(trifluoromethyl)phenyl phosphine oxide (mDN6FPPO) (Scheme 1) in a high-pressure reactor (Parr Instrument Co., USA). In one example, 25 g (0.0496 mol) of purified mDN6FPPO, 200 ml of absolute ethanol and 200 mg of Pd/C catalyst were charged into the flame-dried pressure reactor. The hydrogenation was carried out at 50°C under the hydrogen pressure of 100 psi for 24 h at 200 rpm. Quantitative hydrogenation was confirmed by thin layer chromatography. After filtering off the catalyst over celite, the solution was dried by evaporation, affording yellow crystals. mDA6FPPO crystals obtained were recrystallized in water/ethanol (90:10) mixture and further purified by sublimation to obtain white crystals of mDA6FPPO (yield:90%, m.p. 229.7°C by DSC).

2.5. Characterization of monomers

6FPPO, mDN6FPPO and mDA6FPPO were characterized by FT-IR, NMR, elemental analyzer (EA), titrator, and melting point measurements. FT-IR spectra were recorded with KBr pellets and Perkin Elmer IR 2000 spectrometer, while ^{1}H-NMR, ^{31}P-NMR and ^{19}F-NMR spectra were obtained using 300 MHz FT-NMR (JEOL JNM-LA 300 WB). Chemical shifts were given in parts per million with tetramethylsilane as the internal reference for ^{1}H-NMR, H_2PO_3 for ^{31}P NMR and $CFCl_3$ for ^{19}F-NMR, respectively. $CDCl_3$ or deuterated DMSO was used as a solvent. Elemental analysis was carried out with EA-1108 (Carlo Erba Instrument, Italy), while the titration was performed with an Auto-titrator 670 (Metrohm). The melting temperature of monomers was determined with a digital melting point apparatus (Model 1A9100, Fisher) and differential scanning calorimetry (DSC, TA-2910).

2.6. Synthesis and characterization of polyimides

All polyimides were prepared from the two-step route; e.g. synthesizing the poly(amic acid) precursor, followed by solution imidization (Scheme 2 (synthesis of polyimide via two-step route)). The number-average molecular weight was controlled to 20,000 g/mol by adding mono-functional phthalic anhydride (PA). The poly(amic acid) was synthesized in a three-neck round bottom flask equipped with a mechanical stirrer, reverse Dean–Stark trap, condenser, drying tube, and nitrogen inlet with a thermometer. After flame drying the apparatus under nitrogen flow, the diamine monomer was first charged to the flask followed by distilled NMP.

Upon complete dissolution of diamine, PA and dianhydride were added. The mixture was reacted for 24 h at room temperature at 15 wt.% solid concentration. The solution

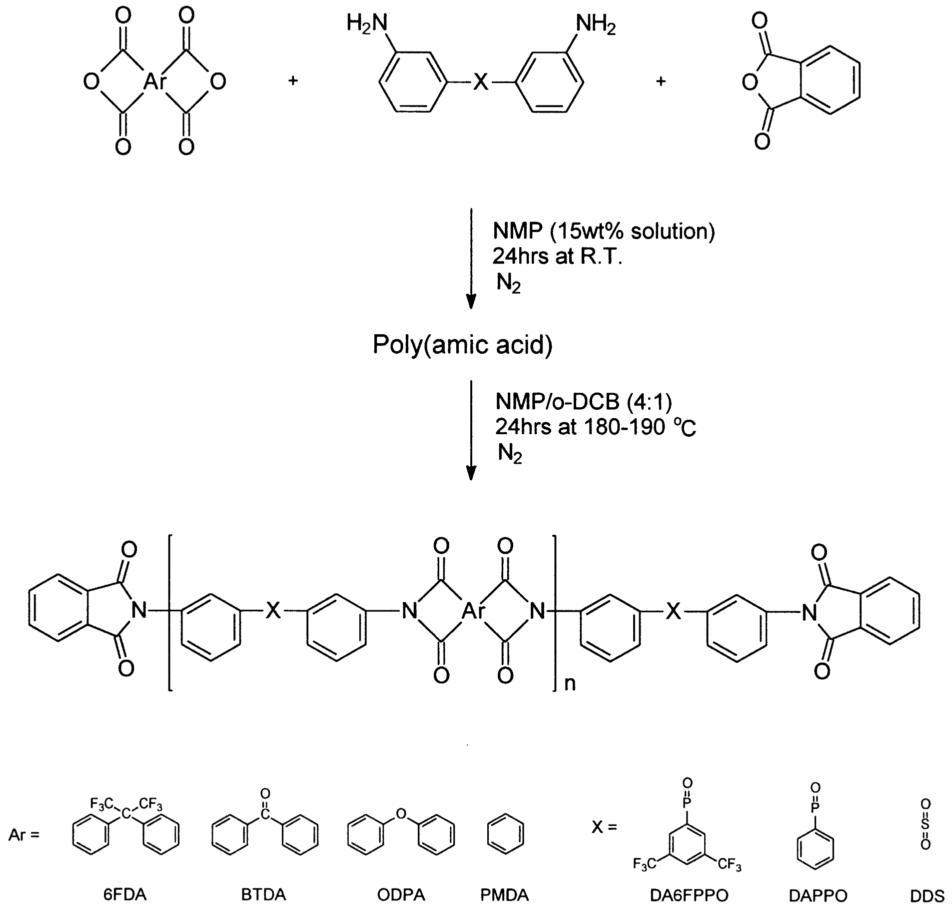

Scheme 2.

imidization was carried out with an azeotroping agent *o*-DCB (20 v/v%) at 180–190°C for 24 h under nitrogen flow. The reaction mixture was then cooled to room temperature and isolated into water–methanol mixture, followed by filtration and drying. After redissolving the polymer in chloroform, it was precipitated, filtered and vacuum dried at elevated temperatures.

The polyimides were analyzed by FT-IR (IR 2000, Perkin Elmer) and FT-NMR (300 MHz, JEOL) and further characterized via thermal analysis, intrinsic viscosity measurements and optical property measurements. The solubility was determined by dissolving the polyimide film in a solvent at a concentration of 10 wt.% at room temperature for 24 h. Intrinsic viscosities were measured with a Canon Ubbelohde viscometer in NMP at 25°C. The polyimides, which showed good solubility in THF were subjected to GPC analysis (Waters M38003, M515).

The thermal properties were measured via differential scanning calorimetry (DSC, TA-2910) and thermogravimetric analyser (TGA, TA-2980) in air or nitrogen at a heating rate of 10°C/min, respectively. A dynamic mechanical analyzer (DMA, TA-938) was also utilized to measure the T_g of the samples, using specimen, which had dimensions of $10 \times 5 \times 0.05\ \mathrm{mm}^3$ in a resonance mode. The refractive indices of polyimides were measured using thin films on silicon wafer with a Metricon Prism Coupler (Model 2010) with 1.55 μm laser diode. The thin film was prepared by spin coating polyimide solution in TCE. The in-plane (n_{TE}) and out-of-plane (n_{TM}) refractive indices of polyimides were measured by a prism coupler and the birefringence ($n_{\mathrm{TE}} - n_{\mathrm{TM}} = \Delta n$) was calculated.

2.7. Adhesive properties of polyimides

The adhesive properties of polyimides were evaluated using bare or Cr/silane-coated Cu foil, which had a thickness of 0.035 mm. The bare Cu foils were etched for 20 s in a solution prepared from 60 parts by volume (pbv) sulfuric acid, 15 pbv hydrogen peroxide and 2000 pbv deionized water. Foils were then rinsed with deionized water and dried at 100°C for 30 min. However, the Cr/silane-coated Cu foil was used without further treatment. Cu foils were coated with 15 wt.% polyimide solution in DMAc and dried at 100°C for 30 min. The coating was repeated to obtain a thickness of 0.01 mm, then further dried at 150°C for 1 h and at 300°C for 30 min.

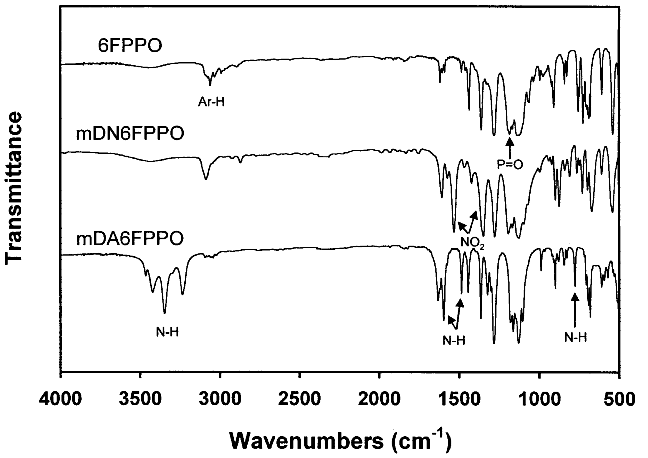

Fig. 1. FT-IR of mDA6FPPO.

T-peel test specimens were prepared by sandwiching the two polyimide-coated Cu foils, following ASTM D 1876-95. Bonding conditions such as temperature and holding time were optimized with the polyimides of BTDA–mDDS. The samples were heated to T_g + 20°C at a heating rate of 7°C/min under contact pressure, then further heated to T_g + 30, T_g + 50, or T_g + 70°C at 1500 psi. After holding for 10, 20, or 30 min, the samples were cooled to room temperature under pressure. The samples were cut into 25.4 mm × 250 mm dimensions, and tested via T-peel test at room temperature with an Instron 5567 at a cross-head speed of 2.54 cm/min. The peel strength was measured from at least 150 mm of the sample after discarding the data from initial 50 mm. At least six test specimens were tested for each polyimide and results were averaged. The failure surfaces were also analyzed by SEM to elucidate the adhesion mechanism.

3. Results and discussion

3.1. Synthesis and characterization of mDA6FPPO

mDA6FPPO was prepared by nitration of 6FPPO to mDN6FPPO, followed by hydrogenation. After purification at each step, the yield was 85% for 6FPPO, 95% for mDN6FPPO and 90% for mDA6FPPO, resulting in an overall yield of 72.7%, compared to the overall yield of 30% for mDAPPO [33]. The monomers were either white crystals (6FPPO, mDA6FPPO) or pale yellow crystals (mDN6FPPO) and exhibited a very narrow melting point range, indicating high purity: 94.2–95.1°C (6FPPO); 174.5–175.0°C (mDN6FPPO) and 225.5–226.5°C (mDA6FPPO). The high yield of mDA6FPPO could be due to the excellent stability of 3,5-bis(trifluoromethyl) phenyl magnesium bromide in THF at room temperature, which was at least 48 h as confirmed by gas chromatography. Another likely possibility is that the strong electron-withdrawing nature of trifluoromethyl moieties in mDA6FPPO, facilitating the third ring, thus preventing the formation of trinitro compounds.

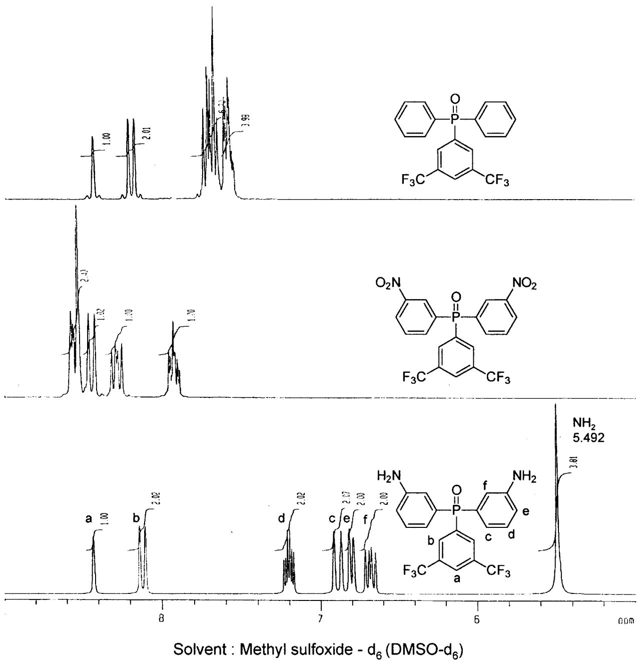

Fig. 2. ^{1}H-NMR of mDA6FPPO.

The chemical structures of 6FPPO, mDN6FPPO and mDA6FPPO were identified by FT-IR, ^{1}H-NMR, ^{31}P-NMR and ^{19}F-NMR, while mDA6FPPO was further characterized by elemental analyzer and titration of the amine groups. In the IR spectrum of 6FPPO, P=O stretching absorption appeared at 1187 cm^{-1}, while C–F multiple stretch bending absorptions from trifluoromethyl groups were observed between 1300 and 1100 cm^{-1} (Fig. 1). mDN6FPPO exhibited the nitro absorption peaks at 1534 and at 1350 cm^{-1} from NO_2 asymmetric and symmetric stretching, respectively, which were not observed from 6FPPO. In addition, P=O stretching absorption peak was observed at 1195 cm^{-1} with mDN6FPPO, compared to that at 1187 cm^{-1} with 6FPPO because of the electron-withdrawing effect of nitro groups. However, mDA6FPPO showed typical N–H stretching absorptions at 3423 and 3347 cm^{-1}, N–H bending at 1598 cm^{-1} and N–H out-of plane bending at 778 cm^{-1} due to the amine groups. P=O stretching appeared at 1182 cm^{-1}, a slightly lower wavenumber than that with 6FPPO (1187 cm^{-1}) and mDN6FPPO (1195 cm^{-1}), which was influenced by the electron-donating effect of diamine.

In the ^{1}H-NMR (300 MHz, DMSO-d_6) spectrum of 6FPPO, protons in 3,5-bis(trifluoromethyl)phenyl moiety appeared at 8.44 ppm (triplet, 1H) and 8.20 ppm (quartet, 2H), while protons in diphenyl moiety appeared at 7.68 ppm (multiplet, 6H) and 7.59 ppm (multiplet, 4H) (Fig. 2). By nitrating 6FPPO, four groups of peaks were observed from mDN6FPPO: 8.53–8.57 ppm (multiplet, 5H); 8.44 ppm (doublet, 2H); 8.28 ppm (quartet, 2H) and

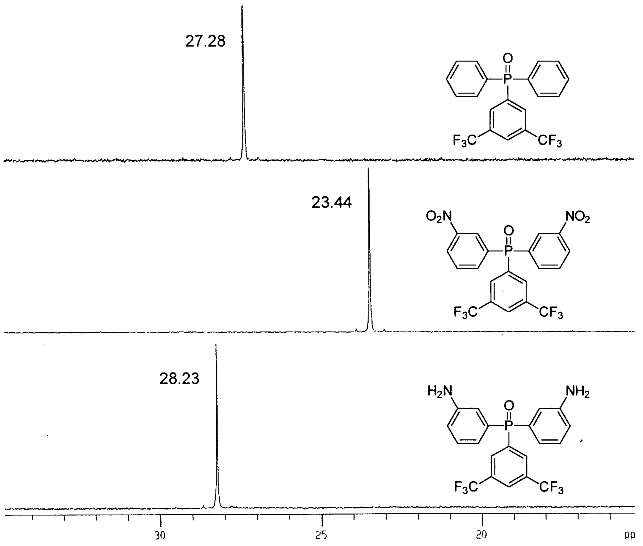

Solvent : Chloroform-d ($CDCl_3$) Reference : H_3PO_4 at 0 ppm

Fig. 3. ^{31}P NMR of mDA6FPPO.

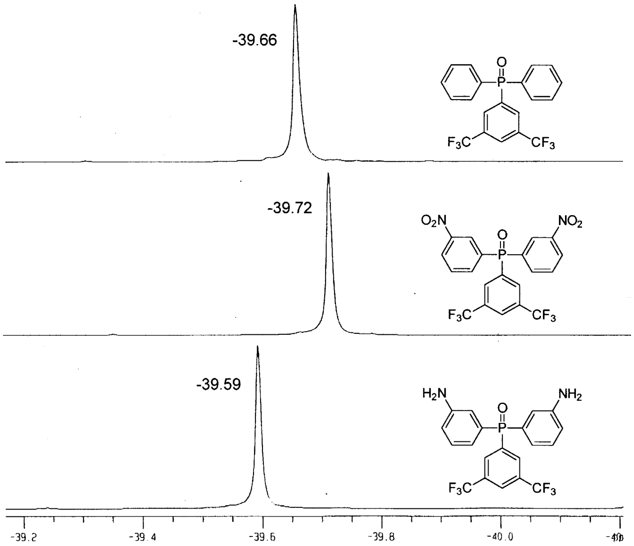

Solvent : Chloroform-d ($CDCl_3$) Reference : $CFCl_3$ at 0 ppm

Fig. 4. ^{19}F NMR of mDA6FPPO.

7.92 ppm (multiplet, 2H). The hydrogen peaks from the nitro phenyl moieties were shifted downfield, compared with those of 6FPPO, owing to the deshielding effect of electron-withdrawing nitro groups [34]. However, the peak shift of protons in 3,5-bis(trifluoromethyl)phenyl pendant group was relatively small, possibly due to the distance from the electron-withdrawing nitro groups.

The electron-donating effect of amino groups in mDA6FPPO was demonstrated by the seven groups of peaks: 8.42 ppm (singlet, 1H) and 8.12 ppm (doublet, 2H) for protons in 3,5-bis(trifluoromethyl)phenyl pendant group; 7.20 ppm (multiplet, 2H); 6.89 ppm (doublet, 2H); 6.80 ppm (doublet, 2H) and 6.67 ppm (quartet, 2H) for hydrogens in amino phenyl moieties, and 5.49 ppm (singlet, 4H) for hydrogens in amino groups (Fig. 2). The hydrogen peaks from amino phenyl moieties were shifted up-field, compared to those of 6FPPO and mDN6FPPO, indicating the shielding effect of the electron-donating amino group [35]. But the shifts of hydrogen peaks from 3,5-bis(trifluoromethyl)phenyl pendant group were again negligible due to the distance from the electron-donating amino functions.

^{31}P NMR (300.4 MHz, $CDCl_3$) analysis provided a sharp single peak at 27.28 ppm for 6FPPO, 23.44 ppm for mDN6FPPO and 28.23 ppm for mDA6FPPO (Fig. 3). As noted, the peak shifted up-field upon oxidation and down-field upon hydrogenation, which is opposite to ^{1}H-NMR results. In ^{19}F-NMR (282.65 MHz, $CDCl_3$), all the peaks were found in similar positions (Fig. 4): −39.66 ppm (6FPPO); −39.72 ppm (mDN6FPPO) and −39.59 ppm (mDA6FPPO), indicating that F was not affected by oxidation and hydrogenation, as expected from ^{1}H-NMR. However, sharp single peaks indicate high purity of monomers.

Table 1
Elemental analysis of diamines

	mDA6FPPO		mDAPPO	
	Calculated (wt.%)	Measured (wt.%)	Calculated (wt.%)	Measured (wt.%)
Carbon	54.06	54.02	70.12	70.06
Hydrogen	3.40	3.38	5.56	5.51
Nitrogen	6.30	6.30	9.09	9.08

Further characterization of mDA6FPPO and mDAPPO by elemental analysis and titration provided experimental results, which were well matched to the theoretical values, confirming the successful synthesis of high-purity monomers (Tables 1 and 2). The measured wt% of C, H and N were 54.02, 3.38 and 6.30, in excellent agreement with the theoretical values: 54.06, 3.40 and 6.30 for mDA6FPPO. Elemental analysis of mDAPPO also showed very good agreement between calculated and measured values (Table 1). The molecular weight of mDA6FPPO measured by titration is 444.50 g/mol compared to 444.04 g/mol by EA and 444.31 g/mol by theoretical calculation, exhibiting excellent agreement (Table 2). The characterization of

Table 2
Characteristics of diamines

	MW (g/mol)			m.p. (°C)		Color
	Calculated	Measured		MPA[a]	DSC	
		EA[b]	Titrator			
mDA6FPPO	444.31	444.04	444.50	226.0	229.7	White
mDAPPO	308.31	307.95	309.02	203.0	210.6	White

[a] By melting point apparatus.

[b] Elemental analyzer.

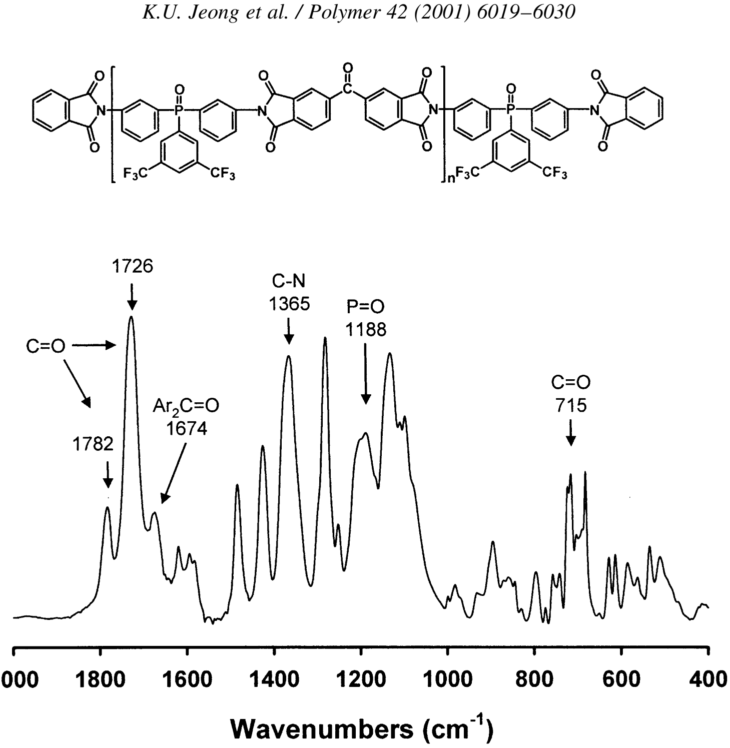

Fig. 5. FT-IR of polyimide from BTDA–mDA6FPPO.

mDA6FPPO via titration and EA revealed that the monomer was successfully synthesized.

4. Synthesis and characterization of polyimides

4.1. Structure of polyimides

Fully imidized polyimides were characterized by FT-IR, ^{1}H-NMR, ^{31}P-NMR and ^{19}F-NMR. The IR spectra of BTDA–mDA6FPPO–PA polyimide showed imide carbonyl peaks at 1782 cm^{-1} (C=O asymmetric stretching), at 1726 cm^{-1} (C=O symmetric stretching) and at 715 cm^{-1} (C=O banding), with the C–N peak at 1365 cm^{-1}, but no amide–carbonyl peak at 1650 cm^{-1}, suggesting complete imidization (Fig. 5). As expected, P=O stretching and C–F multiple stretching bands appeared at 1188 cm^{-1} and 1300–1100 cm^{-1}, respectively. The ^{1}H-NMR (300 MHz, $CDCl_3$) spectrum of BTDA–mDA6FPPO polyimide revealed that all hydrogen peaks were in good agreement with the proposed polymer structure (Fig. 6). A single peak was also observed at 23.04 ppm in ^{31}P-NMR (300.4 MHz, $CDCl_3$) and at −39.55 ppm in ^{19}F-NMR (282.65 MHz, $CDCl_3$), respectively, as expected.

The protons in ^{1}H-NMR spectrum of BTDA–mDA6FPPO polyimide were assigned by considering the electron-withdrawing nature of phosphine oxide, carbonyl and trifluoromethyl moieties (in the descending order). The most deshielded proton could be at E (8.28 ppm, doublet, 2H) of phenyl ring attached to phosphine oxide since these protons are affected by two strong electron-withdrawing

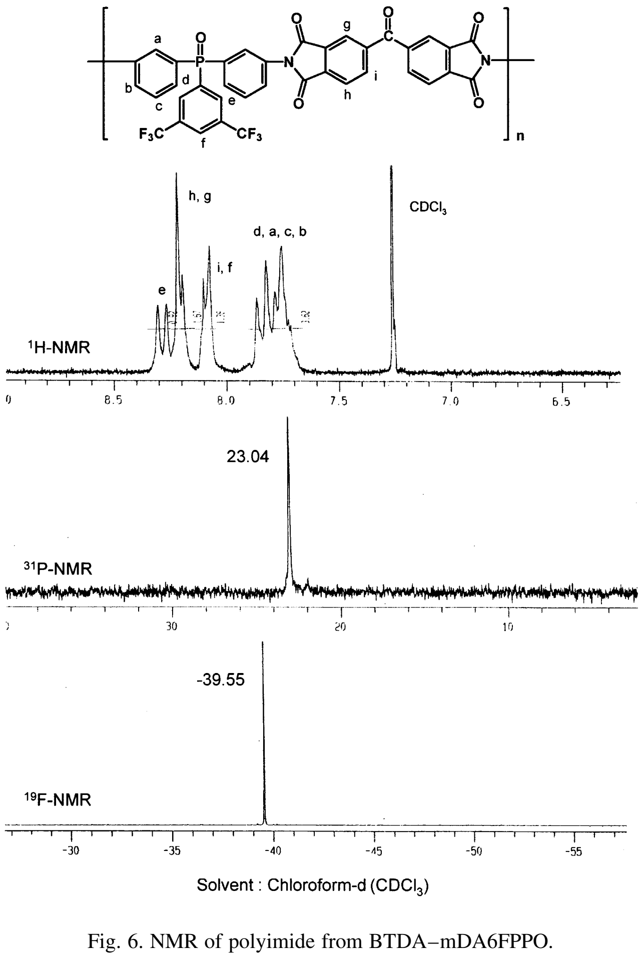

Fig. 6. NMR of polyimide from BTDA–mDA6FPPO.

Table 3
Solubility of polyimides. (At RT for 24 h, S: Soluble, P: Partially soluble, I: Insoluble)

		NMP	DMAc	TCE	$CHCl_3$	THF	Toluene	Acetone
mDA6FPPO	6FDA	S	S	S	S	S	I	S
	BTDA	S	S	S	S	P	S	I
	ODPA	S	S	S	S	S	P	I
	PMDA	S	S	S	S	P	I	I
mDAPPO	6FDA	S	S	S	S	S	I	P
	BTDA	S	S	S	S	I	S	I
	ODPA	S	S	S	S	P	I	I
	PMDA	S	S	S	P	I	I	I
mDDS	6FDA	S	S	P	P	I	I	I
	BTDA	S	S	I	I	I	I	I
	ODPA	S	S	I	I	I	I	I
	PMDA	I	I	I	I	I	I	I

groups such as phosphine oxide and trifluoromethyl moieties. Next deshieled protons are G and H (8.20 ppm, doublet, 4H), and I and F (doublet, 3H) from BTDA. The protons at G, H and I are between two carbonyl groups, but G is more strongly affected, followed by H and I, which are at *meta*- and *ortho*-positions, respectively. The protons between two trifluoromethyl moieties (F) have weaker shielding effect than those between two carbonyl groups. The least deshielded protons are A, B, C and D (7.87–7.75 ppm, multiplet, 8H) in phenyl groups attached to phosphine oxide and they are only affected by phosphine oxide (electron-withdrawing group) and imide groups (electron-donating moiety). Integration of proton peaks (2.00:3.66:3.10:7.88) in ^{1}H-NMR (300 MHz, $CDCl_3$) spectrum of BTDA–mDA6FPPO was in good agreement with the numbers of hydrogen (2:4:3:8) in the of polymide structure.

4.2. Solubility and solution viscosity of polyimides

The solubility of polyimides was greatly enhanced by the incorporation of phosphine oxide moiety and further by trifluoromethyl phenyl group (Table 3). mDDS-based polyimides showed solubility only in NMP and DMAc, but mDAPPO-based polyimides were soluble in NMP, DMAc, TCE and $CHCl_3$, while some mDA6FPPO-based polyimides exhibited solubility even in THF, toluene and acetone. The excellent solubility of mDA6FPPO-based polyimides could be attributed to the presence of bulky CF_3 groups, leading to increased free volume, and also to the phosphine oxide segments providing strong intermolecular forces with solvent molecules [32]. However, polyimides from PMDA–mDDS was insoluble even in NMP, owing to the rigid structure of pyromellitic dianhydride.

Table 4
Characteristics of polyimides

		$[\eta]$[a] (dl/g)	T_g (°C)		T_d (°C)[b]		Residue (wt.%)[c]	
			DSC[d]	DMA[e]	In air	In N_2	In air	In N_2
mDA6FPPO	ODPA	0.22	228	236	533	546	10	55
	BTDA	0.28	243	253	530	532	5	58
	6FDA	0.24	247	257	517	521	3	50
	PMDA	0.20	281	292	522	530	5	53
mDAPPO	ODPA	0.27	251	263	526	532	13	56
	BTDA	0.30	273	285	506	510	23	60
	6FDA	0.29	271	280	524	527	5	60
	PMDA	0.20	331	340	479	479	50	67
mDDS	ODPA	0.23	250	258	557	557	0	57
	BTDA	0.26	266	275	548	551	0	59
	6FDA	0.24	268	281	532	536	0	59

[a] At 25°C in NMP.
[b] By TGA, 5 wt.% loss.
[c] By TGA, at 800°C.
[d] Second heat at 10°C/min in N_2.
[e] 5°C/min, resonance mode.

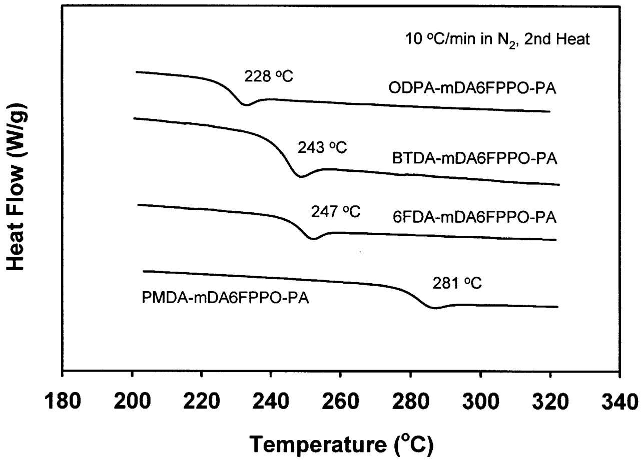

Fig. 7. DSC thermogram of mDA6FPPO-based polyimides.

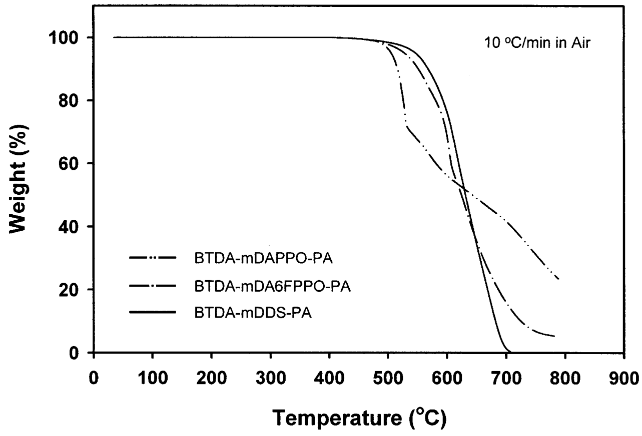

Fig. 8. Effect of diamine on the thermal stability of polyimides.

Since most of the polyimides prepared in this investigation showed good solubility in NMP, the intrinsic viscosity was measured in NMP at 25°C. The intrinsic viscosity of mDA6FPPO-based polyimides ranged from 0.20 to 0.28 dl/g, suggesting a reasonably high molecular weight (Table 4). The intrinsic viscosities of mDAPPO-based and mDDS-based polyimides were in the range of 0.20–0.30 dl/g and 0.23–0.26 dl/g, respectively, which were similar to 0.20–0.28 dl/g of mDA6FPPO-based polyimides. 6FDA–mDA6FPPO polyimide, only polymer which exhibited excellent solubility in THF provided M_n of 22,577 g/mol in GPC analysis. Therefore, the target molecular weight of 20,000 g/mol seemed to be attained, which was further supported by the creasable film formed when polyimides were compression molded with the exception of PMDA–mDDS polyimides. As shown in Table 4, the intrinsic viscosity decreased in the order of BTDA, 6FDA, ODPA and PMDA, which could be related to the stiffness of dianhydride moieties except PMDA and indicated a possible relationship of viscosity to the stiffness of polymer structure and the polymer–solvent interaction. Relatively low intrinsic viscosity of PMDA-based polymides could be attributed to poor solubility.

4.3. Thermal properties of polyimides

mDA6FPPO–PMDA polyimide showed a T_g of 281°C, followed by 247°C (with 6FDA), 243°C (with BTDA) and 228°C (with ODPA) (Fig. 7). DMA analysis resulted in a slightly higher T_g than DSC, but showed a similar trend (Table 4). mDA6FPPO-based polyimides showed lower T_g than mDAPPO-based polyimides and mDDS-based polyimides. This could be attributed to high free volume present in mDA6FPPO, due to bulky CF_3 moieties and non-coplanarity of mDA6FPPO compared to mDAPPO [29].

Among the polyimides, mDAPPO-based polyimide showed the highest char yield (5–50 wt.%) at 800°C, followed by mDA6FPPO-based (3–10 wt.%) and mDDS-based polyimides (0 wt.%), but the initial decomposition temperature of all polyimides in air was at around 500°C (Table 4). The high char yield from mDAPPO-based polyimides can be explained by higher P content (5.23 wt.% for BTDA–mDAPPO) than 4.24 wt.% (BTDA–mDA6FPPO) and 0 wt.% (BTDA–mDDS) polyimides, which resulted in the formation of phosphorus-rich residue from decomposition of phosphine oxide, which covered polyimide and thus delayed decomposition [32].

As shown in Fig. 8, mDDS–BTDA polyimide exhibited the highest initial decomposition temperature (548°C), but the lowest char yield at 800°C (0 wt.%), while mDAPPO–BTDA polyimide showed the lowest initial decomposition temperature (506°C) but the highest char yield (23 wt.%). On the other hand, the polyimide from mDA6FPPO–BTDA, containing fluorine and phosphine oxide, exhibited similar decomposition behavior as mDDS–BTDA polyimide, but slightly lower initial decomposition temperature (530°C) and higher char yield (5 wt.%) at 800°C.

The polyimides from mDA6FPPO and ODPA, PMDA or BTDA exhibited very similar degradation behavior up to 600°C, but slightly different char yield at 800°C. However, 6FDA–mDA6FPPO polyimide exhibited much lower initial decomposition temperature, faster degradation behavior at around 600°C, and lower char yield at 800°C than the polyimides from ODPA, PMDA or BTDA as shown in Fig. 9. The poor thermal stability of 6FDA–mDA6FPPO polyimide could be explained by poor thermal stability of fluorine moiety on 6FDA [36].

4.4. Optical properties of polyimides

In-plane (n_{TE}) refractive index of 1.5351 and out-of-plane (n_{TM}) refractive index of 1.5340 were obtained from 6FDA–mDA6FPPO polyimide (Table 5), compared to 1.5805 (n_{TE})

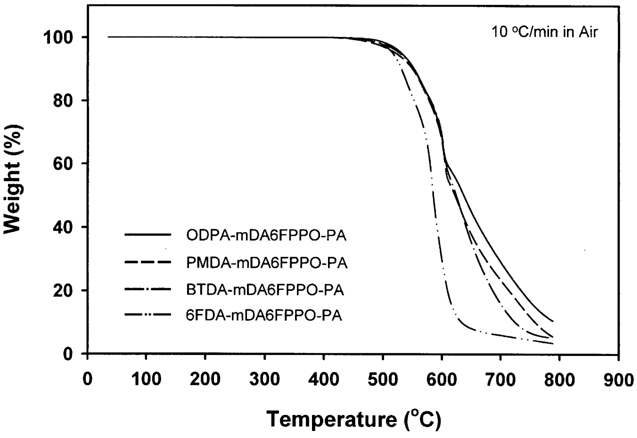

Fig. 9. Effect of dianhydride on the thermal stability of polyimides.

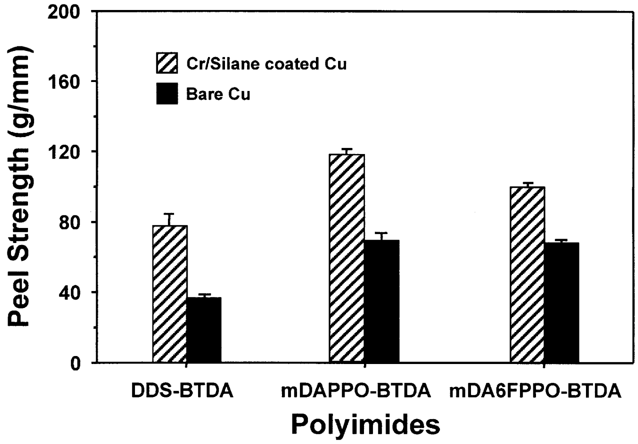

Fig. 10. Effect of diamine on the peel strength of polyimides.

and 15787 (n_{Tm}) for 6FDA–mDAPPO polyimide, 1.5836 (n_{TE}) and 1.5803 (n_{TM}) for BTDA–mDA6FPPO, and 1.5835 (n_{TE}) and 1.5818 (n_{TM}) for ODPA–mDA6FPPO polyimide. Thus, the calculated birefringence was 0.0011 for 6FDA–mDA6FPPO, 0.0017 for 6FDA–mDAPPO, 0.0017 for ODPA–mDA6FPPO and 0.0033 for BTDA–mDA6FPPO polyimides. As expected, 6FDA–mDA6FPPO polyimide exhibited lower refractive index and birefringence than any other polyimides prepared in this investigation, owing to high fluorine content (26.78 wt.%), which is from the pendant 3,5-bis(trifluoromethyl) phenyl moiety as well as from 6FDA.

The refractive index and birefringence of 6FDA–mDA6FPPO polyimide could be compared to those of 6FDA–TFDB polyimide in the literature [16]. As noted, 6FDA–TFDB polyimide exhibited a higher refractive index (1.548 vs 1.5345) and birefringence (0.0066 vs 0.0011) than 6FDA–mDA6FPPO polyimide, despite the higher fluorine content (31.3 vs 26.78 wt.%). This unusual behavior could be explained by the non-coplanarity of phosphine oxide moiety in mDA6FPPO [29]. High fluorine content of 6FDA–mDA6FPPO (26.78 wt.%) might be responsible for the low refractive index, while other polyimides having similar fluorine content exhibited similar refractive indices and birefringence, except BTDA–mDA6FPPO (Table 5). Therefore, it can be said that the effect of the both CF_3 groups may be dependent on the structural backbone of the polyimide.

Table 5
Refractive indices of polyimides (measured at 1.55 μm with 2.5–3.0 μm thick film)

		F (wt.%)	n_{TE}	n_{TM}	$n_{\mathrm{TE}} - n_{\mathrm{TM}}$
mDA6FPPO	6FDA	26.78	1.5351	1.5340	0.0011
	BTDA	15.60	1.5836	1.5803	0.0033
	ODPA	15.87	1.5835	1.5818	0.0017
mDAPPO	6FDA	15.15	1.5805	1.5787	0.0017
	BTDA	–	1.6432	1.6418	0.0014
	ODPA	–	1.6432	1.6408	0.0024
	PMDA	–	1.6827	1.6800	0.0027

4.5. Adhesive properties

The adhesive strength of polyimides was evaluated via T-peel test (ASTM D 1876-95) and the bondline thickness of the samples was approximately 0.02 ± 0.002 mm. The optimized bonding conditions with BTDA–mDDS polyimides were $T_g + 50°C$ (316°C) (bonding temperature) for 20 min (holding time). These conditions were utilized for other polyimides. A higher bonding temperature such as $T_g + 70°C$ led to much lower peel strength, possibly owing to the degradation of adhesives, as well as the oxidization of Cu foils. The highest peel strength (118 g/mm) was obtained from the polyimide of BTDA–mDAPPO, followed by BTDA–mDA6FPPO (100 g/mm) and BTDA–mDDS polyimides (78 g/mm). These results were obtained from samples with Cr/silane-coated Cu foils (Fig. 10). The samples using bare Cu foils also showed a similar trend, but much lower peel strength.

The results clearly suggest that the presence of phosphine oxide moiety enhances peel strength as evidenced by the higher values obtained from BTDA–mDAPPO and BTDA–mDA6FPPO, compared to polyimides without the phosphine oxide moiety (BTDA–mDDS). Also the presence of fluorine slightly lowers the peel strength as indicated by the higher value obtained with BTDA–mDAPPO polyimide than with BTDA–mDA6FPPO polyimide, which contains both phosphine oxide and fluorine. The failure surface analysis by SEM revealed that ductile cohesive failure from the samples containing phosphine oxide moiety (BTDA–mDAPPO) or approximately 90% cohesive failure from the samples containing phosphine oxide and fluorine moiety (BTDA–mDA6FPPO). In comparison, BTDA–mDDS polyimide exhibited less than 50% of cohesive failure, which was estimated by measuring the area covered by polymer layer from SEM micrographs (Fig. 11).

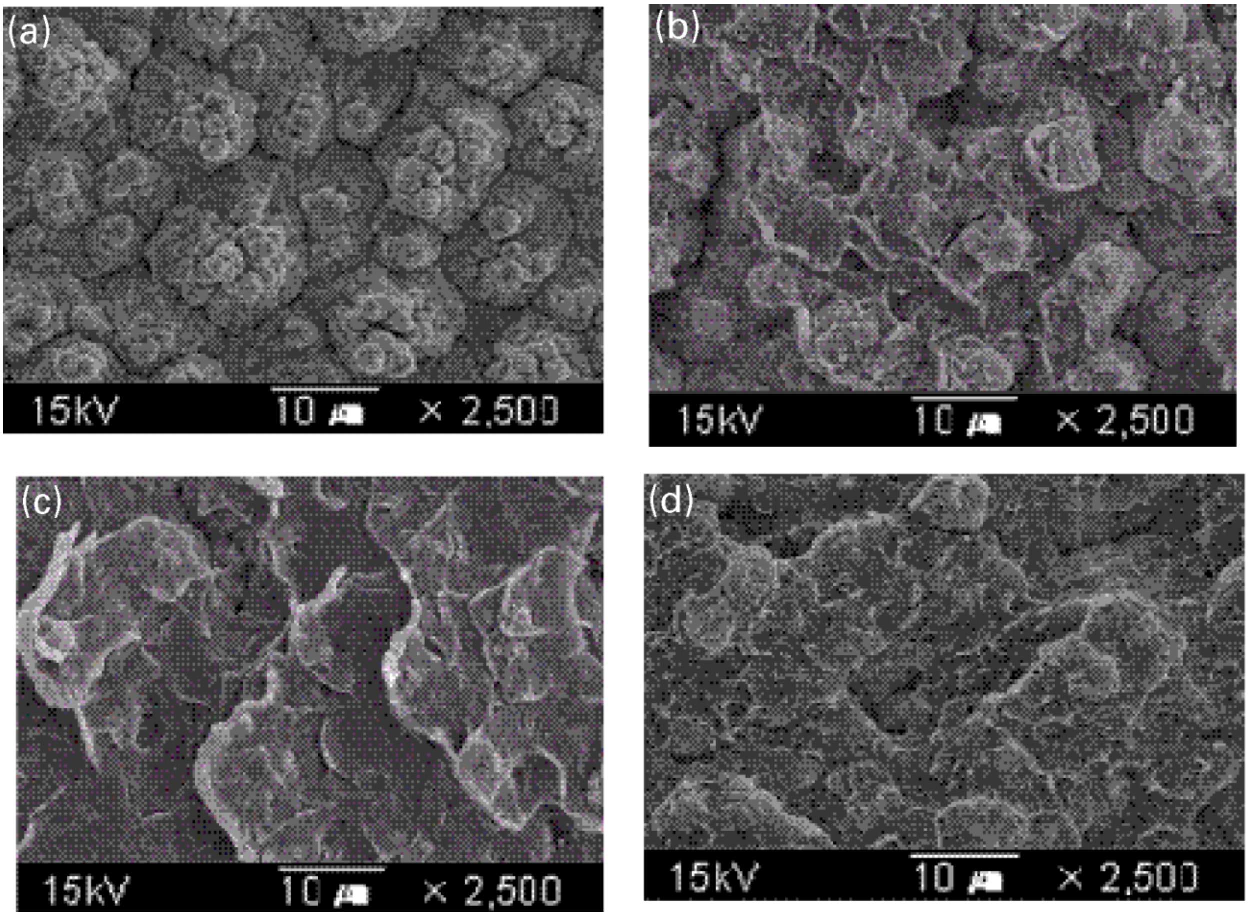

Fig. 11. SEM micrographs of peel test samples with Cr/silane coated Cu foil: (a) as-received Cu foil; (b) BTDA–mDDS polyimide; (c) BTDA–mDAPPO polyimide; (d) BTDA–mDA6FPPO polyimide.

5. Conclusions

1. A novel diamine, containing phosphine oxide and fluorine, mDA6FPPO (bis(3-aminophenyl)-3,5-bis(trifluoromethyl)phenyl phosphine oxide), was successfully synthesized via the Grignard reaction from diphenylphosphinic chloride and 3,5-bis(trifluoromethyl) bromobenzene, followed by nitration and reduction.
2. Polyimides prepared from mDA6FPPO and dianhydrides such as 6FDA, BTDA, ODPA or PMDA exhibited excellent solubility, high T_g (228–281°C) and good thermal stability.
3. Polyimides from 6FDA–mDA6FPPO provided low refractive indices and very small birefringence (0.0011) possibly due to the bulky 3,5-bis(trifluoromethyl)phenyl pendent groups and non-coplanarity of mDA6FPPO, as well as CF_3 moieties in the 6FDA monomer.
4. BTDA–mDA6FPPO polyimde exhibited higher peel strength with Cr/silane-coated Cu foils than BTDA–mDDS polyimides, but lower than BTDA–mDAPPO polyimides, demonstrating the positive effect of phosphine oxide but adverse effect of fluorine on adhesion.

References

[1] Fegar C, Hojasteh MM, McGrath JE, editors. Polyimides: materials, chemistry, and characterization. Amsterdam: Elsevier, 1989.

[2] Wilson D, Stenzenberger HD, Hergenrother PM, editors. Polyimides. New York: Chapman & Hall, 1990.

[3] Fegar C, Khojasteh MM, Htoo MS, editors. Advances in polyimide science and technology. New York: Technomic Publishing, 1991.

[4] Ghosh MK, Mittal KL, editors. Polyimides: fundamentals and applications. New York: Marcel Dekker, 1996.

[5] Feger C, Franke H. In: Ghosh MK, Mittal KL, editors. Polyimides: fundamentals and applications. New York: Marcel Dekker, 1996. p. 759–814.

[6] Bresnock FJ. Thin Solid Film 1988;166:69–78.

[7] Sasaki S, Nish S. In: Ghosh MK, Mittal KL, editors. Polyimides: fundamentals and applications. New York: Marcel Dekker, 1996. p. 71–120.

[8] St. Clair AK, St. Clair TL, Winfree WP. Polym Mater Sci Engng 1988;59:29–32.

[9] Ichino T, Sasaki S, Matsuura T, Nishi S. J Polym Sci, Part A: Polym Chem 1990;28:323.

[10] Matsuura T, Hasuda Y, Nishi S, Yamada N. Macromolecules 1991;24(18):5001–5.

[11] Cheng SZD, Arnold JFE, Zhang A, Hse SLC, Harris FW. Macromolecules 1991;24(21):5856–62.

[12] Matsuura T, Ishizawa M, Hasuda Y, Nishi S. Macromolecules 1992;25(13):3540–5.

[13] Misra AC, Tesoro G, Hougham G, Pendhackar SM. Polymer 1992;33(5):1078–82.

[14] Feiring AE, Auman BC, Wonchoba ER. Macromolecules 1993; 26(11):2779–84.

[15] Brink MH, Brandom DK, Wilkes GL, McGrath JE. Polymer 1994; 35(23):5018–23.

[16] Ando S, Matuura T, Sasaki S. Chemtech 1994;December:20–7.

[17] Yang JW, Wang CS. Polymer 1999;40:1411–9.

[18] Hedrick JL, Labadie J, Russerll TP, Wkarakhar V, Hofer D. Polymer 1993;34(22):4717–26.

[19] Lakshmanan P, Srinivas S, Wilkes GL, McGrath JE. Polym Prepr 1995;36(1):264–5.

[20] Hedrick JL, Chalier Y, Dipietro RA, Jayaraman S, McGrath JE. J Polym Sci, Part A: Polym Chem 1996;34:2867–77.

[21] Carter KR, Dipietro RA, Sanchez MI, Russel TP, Lakshmanan P, McGrath JE. Chem Mater 1997;9(1):105–18.

[22] Hedrick JL, Cha HJ, Miller RD, Yoon DY, Brown HR, Srinivasan S, Di Pietro R, Cook RF, Hummel JP, Klaus DP, Liniger EG, Simonyi EE. Macromolecules 1997;30:8512–5.

[23] Kim SM, Yoon DY, Nguyen C, Han J, Jaffe RL. Mater Res Soc Symp Proc 1998;511:69–73.

[24] Critchley JP, Grattan PA, Whitte MA, Pippet JS. J Polym Sci, Part A-1 1972;10:1789–97.

[25] Moy TM, DePorter CD, McGrath JE. Polymer 1993;34(4):819–24.

[26] Buchwalter LP. In: Ghosh MK, Mittal KL, editors. Polyimides: fundamentals and applications. New York: Marcel Dekker, 1996. p. 587–628.

[27] Linde H. J Polym Sci, Part A: Polym Chem 1982;20:1031–41.

[28] Tesoro G, Wu Y. J Adhes Sci Technol 1991;5(10):771–84.

[29] Lee YJ, Gungor A, Yoon TH, McGrath JE. J Adhes 1995;55:165–77.

[30] Meyer GW, Pak SJ, Lee YJ, McGrath JE. Polymer 1995;36(11): 2303–9.

[31] Park YR, Yoon TH, Yuck JI, Lee SG. Polymer (Korea) 1998;22(6): 901–7.

[32] Wang S, Ji Q, Tchatchoua CN, Shultz AR, McGrath JE. J Polym Sci, Part B: Polym Phys 1999;37:1849–62.

[33] Martinez-Nunez MF, Sekharipuram VN, McGrath JE. Polym Prepr 1994;35:709–10.

[34] Pavia DL, Lampman GM, Kriz GS. Introduction to spectroscopy. 2nd ed. New York: Saunders College Publishers, 1996.

[35] Chern YT. Macromolecules 1998;31(6):1898–905.

[36] Hougham G, Cassidy PE, Jones K, Davidson T, editors. Fluoropolymer 2: properties. New York: Plenum Press, 1999. p. 266.